ORIGINAL RESEARCH

Performance of high-density polyethylene–starch–linen fiber biocomposite

Mohammed Zighed[1] · Benamar Benotmane[1]

Abstract

This study was carried out on the physicochemical and mechanical characterization of a biocomposite consisting of high-density polyethylene (HDPE)/starch matrix reinforced with linen fiber which is renewable, inexpensive and biodegradable material. The linen fibers were modified through the alkaline treatment, and the polymers HDPE and starch were blended without compatibilizers. The composites were fabricated using a two-stage process: mixing and thermocompression. Characterizations were analyzed using Fourier transform infrared spectroscopy (FTIR), scanning electron microscopy (SEM), thermogravimetric analysis (TGA), differential scanning calorimetry (DSC), Izod impact, and tensile strength tests. The FTIR spectra and SEM analysis showed weak compatibility between HDPE and starch. Compared to HDPE, the crystallinity of the HDPE/starch blend was enhanced and the thermal stability was reduced as revealed by ATG and DSC analyses. The mechanical Izod impact and tensile tests revealed improved stiffness and Young's modulus with decreased impact strength, tensile stress and elongation-at-break. Alternatively, the HDPE/starch/linen fiber biocomposite exhibited better improved mechanical proprieties while maintaining good crystallinity and thermal stability, on account of the high fracture resistance and reinforcement of the linen. The biocomposite with 60% HDPE, 20% starch, and 20% linen fiber can be considered for use in industrial applications such as manufacturing and packaging, in accordance with economic and environmental requirements.

Keywords Starch · HDPE · Linen fiber · Biocomposite · Degradability

Introduction

Biocomposites are increasingly being used in industrial applications such as automotive, construction, electronics, and packaging, as well as in scientific research as they offer major advantages (renewability, low cost, recyclability and biodegradability) [1]. Biocomposites are reinforced polymeric materials in which at least one constituent, the matrix or the fiber is bio-based or biodegradable [2].

The matrix consists of a polymer or blend of polymers and the fibers are based on natural resources, which are biodegradable and renewable materials. The plastic matrix serves as an adhesive to maintain the fibers in place, provide strength and stiffness to the structure, so that appropriate

structural components can be manufactured [3]. On the other hand, fibers are considered as load bearing constituents in composite materials [1]. Many authors have highlighted the difficulty in substituting petroleum-based materials in terms of both cost and performance. A sustainable approach is to combine the major characteristics and benefits of plastics and bioresources into a cost-effective bio-based product [3, 4]. Furthermore, substituting the synthetic polymers by biodegradable biopolymers contribute largely in fighting against the plastic pollution [5].

Apart from the environmental concerns, polymeric materials have contributed to significant improvements. Some polymers, such as polyolefins in particular, are easy to process and their low price, combined with their good chemical and physical properties, have made them the most widely used resins for packaging and a multitude of plastic applications. The most widely used commodity thermoplastic is polyethylene (PE), which is produced with different morphology and crystallinity degrees: 34 to 62% for linear low-density polyethylene (LLDPE), 42 to 62% for low-density

✉ Mohammed Zighed
   m.zighed@univ-boumerdes.dz

1   Research Unit of Materials, Processes and Environment
    (URMPE), Faculty of Technology, M'Hamed Bougara
    University, Boumerdes, Algeria

polyethylene (LDPE), and 62 to 82% for high-density polyethylene (HDPE) [6, 7]. It is also worth noting that the development of a biodegradable plastic based on PE has been the concern of many studies [8–10]. The fully biodegradable materials have proven to have limited industrial application due to their low mechanical and chemical strength and limited availability. Particularly, PE-based biocomposites offer an alternative by significantly reducing the amount of plastics through partial degradation [3]. In this respect, starch, as a low-cost but efficient biodegradable material, is attractive for use in polymer blends with other synthetic materials [10, 11]. Starch has also a wide range of applications in different industries [12]. It has been reported that starch can be added to HDPE using deep eutectic solvents to form HDPE-derived biocomposites and thus makes the material rapidly degradable [13]. As highlighted in many previous studies, to improve the composition and the contribution of biomaterials in the composite, natural fibers can also be blended with HDPE/starch [10, 11]. Thus, the composite is more environmentally friendly, the amount of PE introduced into the final material is reduced and the loss of mechanical properties caused by the replacement of PE by starch is compensated. Natural fibers are relatively abundant and inexpensive reinforcements for polymers blends and can provide green and sustainable biocomposites. Furthermore, these renewable fibers have good mechanical properties [14], providing the opportunity to add these fibers to blends as reinforcements for composites due to their superior stiffness and strength [15]. In addition, natural fibers replacing synthetic fibers increase the crystallinity of the polymer matrix [16]. Flax, jute, sisal and kenaf are the most widely used natural fibers for reinforcement [17]. Micro-winceyette fiber, sugarcane fiber, cotton fiber, eucalyptus fiber, cassava bagasse cellulose, wheat straw fiber and sisal fiber have been also widely used for the same aim [18]. Linen fibers, which belong to bast fibers family and derived from the stems of flax plant have a high tensile strength and are used for polymeric composites reinforcement [19]. Moreover, linen fibers have an excellent absorption moisture absorption and considerable breaking strength characteristics [20]. These fibers are low-cost alternatives to synthetic fibers [21].

However, the problem encountered in matrix-fibers is related to the interfacial adhesion because of the hydrophobicity of many thermoplastics and the hydrophilicity of fibers. To overcome this constraint, various fibers' treatments could be applied such as alkali treatment [14]. The alkali treatment of natural fibers removes moistures and impurities and improves the mechanical proprieties of the fibers [22]. It has been established that the free hydroxyl groups resulting from the breaking of existing hydrogen bonds will contribute to the formation of new bonds with the molecules in the polymer blend [23]. Furthermore, alkalization creates rough areas on the surface of fiber due

to the elimination of impurities and non-cellulosic materials [24]. It was also pointed out that natural fibers are generally used to enhance the composites stiffness and tensile strength. Further features such as elongation-at-failure, thermal stability, adhesion of fibers and matrix, dynamic and long-term behavior, price and processing cost, and environmental considerations are to be taken into account when selecting suitable reinforcement fibers [4]. Different fibers were used in blends of PE/starch as reported in the literature. Curauá fibers were added to thermoplastic starch (TPS)/maleate polyethylene blends improving the material thermal resistance allowing its use as thermal insulators in building [10]. Sisal fibers were successfully incorporated in maleic anhydride grafted HDPE to improve the mechanical properties (tensile strength, tensile modulus, and creep-resistance) of the composite [25]. However, a higher starch content (40 to 60% by weight) in the PE/starch decreased the strength and elongation-at-failure of the composite due to the low interfacial adhesion between the two components [26]. Similar results were obtained for elongation-at-failure of a 60% LDPE/40% TPS composite in contrast to the good degradability achieved [27]. The degradation concerned the TPS whereas PE was subjected to a reduction of molecular weight due to the carbon–carbon backbone cracking as suggested [27]. The resulting increase in the modulus of elasticity and the degree of crystallization of the composite probably supported this finding. It is also worth highlighting the recyclability of the LDPE/TPS composite recorded after 10 reprocessing cycles [7]. Thus, the analysis of the findings of the above referenced studies highlights the performance of PE/TPS/fiber composites in terms of mechanical properties, biodegradability and recyclability.

In the present work, we attempted to prepare a biocomposite based on HDPE/starch blend reinforced with linen fibers by two-steps process: mixing and thermocompression. We investigated the effect of starch and linen fiber contents on the physico-mechanical parameters of the processed composites.

Experimental

Materials

Corn starch was obtained from Biochem Chemopharma, France. 5502 grade HDPE with a density of 0.9545 g/cm^3 at 23 °C and melt flow index of 0.58 g/10 min was obtained from HDPE production unit of the Algerian state oil and Petrochemicals Company Sonatrach. Chemically treated linen fibers with an average length of 5–7 mm were used in this study (fibers from Algeria).

Fiber treatment

Linen fibers were immersed in 4% aqueous NaOH solution during 3.5 h. Then, the fibers were retrieved and washed with distilled water until reaching neutralization (pH 7) and dried in a hot oven for 3 h at 80 °C before use.

Preparation of samples

Samples composed of HDPE and starch for a set and HDPE, starch, and linen fibers for a second set were produced according to the following process:

Mixing

The mixture (HDPE, starch with/without linen fiber) was fed into a two-roll IQAPLAP mixer (Spain). The temperature of the rollers was set at 170 °C and the rollers were rotated in opposite directions, fusing the ternary or binary mixture poured onto the interfacial area between the rollers. After 20 min of mixing and heating to ensure that the mixture was homogeneous, the composite was collected into sheet and cut into small pieces prior to the thermocompression processing. Due to mixing capacity limitations, the maximum fiber content in composite samples was set at 20%.

Thermocompression molding

The samples were hot-pressed using a IQAP LAP hydraulic press (Spain) in two metal containers (molds) 21×21 cm and 2 and 3 mm thickness. The thermocompression was carried out in 5 cycles with the features shown in Table 1. The samples were removed and cooled to room temperature after the cycles of thermocompression were completed. The compositions of the samples are listed in Table 2.

Figure 1 shows samples of thermocompressed composites.

After 48 h, the performed plates were subjected to cut test shapes and kept in sealed bags to be prevented from moisture. Mechanical test specimens of thermocompressed composites are shown in Fig. 2

Table 1 Thermocompression features

Features/cycles	Cycle 1	Cycle 2	Cycle 3	Cycle 4	Cycle 5
Upper and lower plates' temperature (°C)	177	177	80	40	30
Pressure (MPa)	1	5	10	5	0,1
Duration (min)	1	2	7	5	2

Table 2 Compositions of the samples

Sample code	HDPE % (w/w)	Starch % (w/w)	Fiber % (w/w)
P100 S00 F00	100	00	00
P60 S40 F00	60	40	00
P60 S30 F10	60	30	10
P 60 S20 F20	60	20	20

Fourier transform infrared spectroscopy (FTIR)

The IR spectra were obtained from Shimadzu Tracer-100 IR Spectrometer (Japan) equipped with ATR sampling technique (attenuated total reflection) and Lab solution data acquisition system. The composites strips were introduced directly into ATR cell and tested in transmittance mode. The samples were scanned at a frequency range of 4000–600 cm^{-1} with 20 scans and 4 cm^{-1} resolution.

Morphological analysis

The morphological study using a scanning electron microscopy (SEM) FEI model Quanta 650 (FEI Company, USA) with an accelerating voltage of 10 kV was carried out on the fractured surfaces of the samples after the tensile rupture to assess the interfacial structure within the matrix. Prior to examination, the concerned surfaces were coated with metallized layer of 4 nm in thickness. The images' magnification ranged from 257× to 1081×.

Thermal proprieties

Thermogravimetric analysis (TGA)

In studying the thermal degradation and stability of the prepared composites, TGA measurements were carried out using SDT Q 600 instrument (Artisan Technology Group, USA) equipped with a computer for data acquisition (TA Analysis). The samples, which had a weight ranging from 4 to 13 mg, were heated from 25 to 800 °C at a heating rate of 15 °C/min under nitrogen atmosphere (50 mL/min).

Differential scanning calorimetry analysis (DSC)

The differential scanning calorimetry was conducted using a differential scanning calorimeter 131 evo (Setaram KEP Technologies Company, Switzerland), under nitrogen flow of 30 mL/min. Each sample undergoes two heating cycles and two cooling cycles: heated from 25 to 160 °C, then cooled to 25 °C, reheated again from 25 to 160 °C and recooled to 25 °C with heating and cooling rates of 10 °C/min. The samples weight varied from 10 to 20 mg. The values of melting

Fig. 1 Samples of thermocompressed composites: **a** P60 S30 F10 and **b** P40 S60
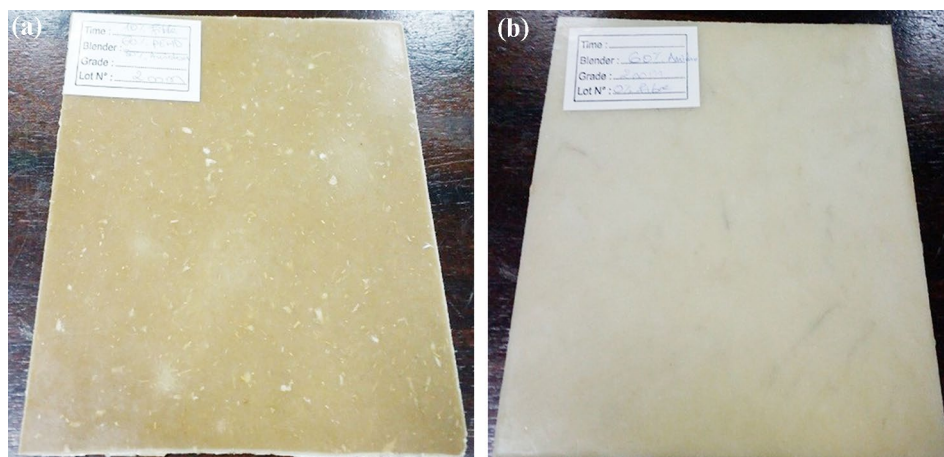

Fig. 2 Shape of mechanical test specimens of thermocompressed composites

temperature (T_m) and enthalpy (ΔH_m) were calculated from the second heating, whereas the crystallization temperature, T_c, and enthalpy (ΔH_c) were calculated from the second cooling from DSC curves.

The bulk crystallinity degree (X_c, %) was calculated using the following equation [27]:

$$X_c = \frac{dH_m}{\%(\mathrm{wt}) \times dH_{m_0}},\tag{1}$$

where %(bywt) is the weight fraction of HDPE and dH_{m_0} is the theoretical enthalpy of 100% crystalline HDPE. dH_{m_0} has been estimated at 293.6 J/g as reported in the literature [28].

Characterization of mechanical properties

Izod impact test

The Izod impact test as a standard method for determining the impact resistance of materials was conducted according to ASTMD D-256 standard using an Izod impact strength tester apparatus: the Resil impactor provided by Ceast

Company (Torino, Italy). Three notched specimens were prepared from composite samples each with a thickness of 3 mm, a width of 12.7 mm, and a notch size of 2.5 mm and tested using a pendulum speed of 2.9 m/s. The average value of the energy required to break the specimen was calculated.

Tensile strength tests

Tensile tests were carried out on three standard specimens according to ISO 527 on a universal testing machine 50 KN (MTS Criterion model 45, France). The stress–strain tests were conducted with a strain rate of 1 mm/min. The tensile stress, Young's modulus, and elongations-at-break were calculated and their average values were considered as the most meaningful.

Results and discussion

Fourier transform infrared spectroscopy (FTIR)

To investigate the type of interaction in HDPE/starch blends and HDPE/starch/fiber composites, FTIR analyses of samples HDPE (P100%), starch (S 100%), P60 S40 and P60 S40 F20 were carried out and are shown in Fig. 3. Table 3 recapitulates the appeared main peaks of the FTIR spectra and their wavenumbers. The characteristics absorbance bands for P100 samples are located at: 2914 cm⁻¹, 2847 cm⁻¹ corresponding, respectively, to asymmetrical and symmetrical stretching vibrations –CH₂ of the methylene group, 1474 cm⁻¹, which is due to the asymmetric deformation vibrations (bending) of the methylene group, and the sharp band of 719 cm⁻¹ due to CH₂ rocking vibrations. The doublet peaks at 1474–1462 cm⁻¹ and 731–719 cm⁻¹ are indicative of the crystallinity of PE [29]. The FTIR spectra of starch illustrates the broad band near 3250 cm⁻¹ corresponding to the stretching of hydrogen bonded O–H groups. Band
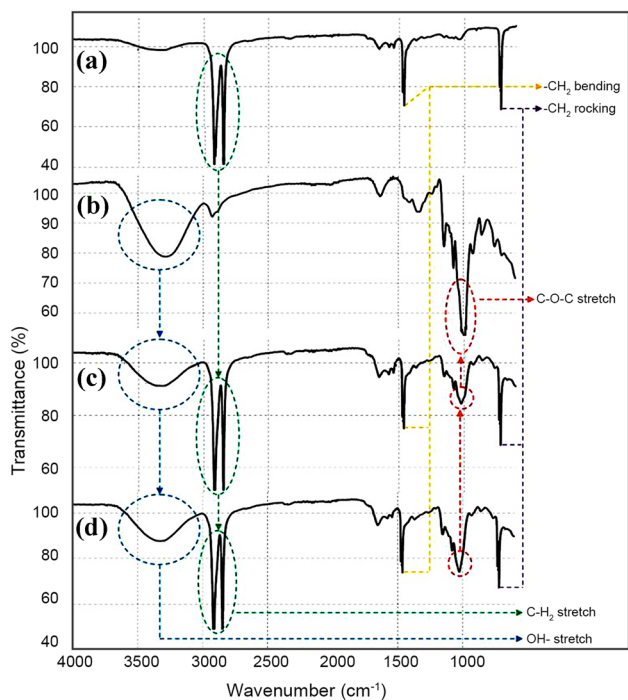
Fig. 3 FTIR spectra of: **a** HDPE, **b** starch, **c** P60 S40 and **d** P60 S20 F20

near 2930 cm^{-1} is attributed with the axial deformation of CH$_2$ group. The peak at 1632 cm^{-1} is characterized by the stretching vibration of H–O–H in water molecules present in hygroscopic materials [30]. The peak at 1337 cm^{-1} corresponds to C–OH bending vibration of starch molecule, and

the characteristic bands observed between 1149 cm^{-1} and 762 cm^{-1} correspond to starch molecule. Several absorbencies are attributed to C–O bond stretching vibrations in the C–O–H groups (1150 cm^{-1}, 1076 cm^{-1}) and in the C–O–C groups (993 cm^{-1}, 860 cm^{-1}, and 762 cm^{-1}) within the anhydroglucose ring of the starch structure. The FTIR spectra of the PE60 S40 and P60 S20 F20 blends are similar revealing the characteristic bands of PE and starch at the same peaks recorded on the previous spectra with slight shifts and varying absorption intensities (Fig. 3c, d and Table 3). Indeed, the absorption intensity of the peaks at 2916 and 2847 cm^{-1} decreased and at 1462 cm^{-1} a small reduction appeared, which clarifies a weakening of the CH$_2$ groups in the PE chains. In addition, the broad and strong absorption in the 3250 cm^{-1} region related to the O–H groups of starch (Fig. 3b), decreased significantly in the presence of PE (Fig. 3c, d), which is indicative of the decrease of starch concentration in the samples and the dispersion of O–H groups between the PE molecular chains. The similarity of chemical structure of starch and lignocellulosic fiber such as linen makes their chemical groups absorb in infrared at similar regions [10]. The uniform dispersion of the starch in the HDPE matrix was achieved, regardless of their immiscibility as evidenced by no shift in the correlative peaks and no change in their shape. These results are consistent with the literature [31].

Morphological analysis

SEM micrographs of tensile fracture surfaces of HDPE/ starch blends and HDPE/starch/linen fibers composites at

Table 3 Peaks' wavenumbers and transmittance intensity of main signals

Main signals	PE 100%		Starch 100%		(PE 60%/starch 40%)		(PE 60%/starch 20%/ fiber 20%)	
	Wavenumber (cm^{-1})	Intensity (%)	Wavenumber (cm^{-1})	Intensity (%)	Wavenumber (cm^{-1})	Intensity (%)	Wavenumber (cm^{-1})	Intensity (%)
O–H stretch	–	–	3250.05	79.21	3332.99	91.17	3336.85	87.84
Symmetric and asymmetric aliphatic C–H$_2$ stretch	2846.93	33	2929.87	92.08	2846.93	46.39	2846.93	43.54
	2914.44	29.88			2916.36	42.86	2916.36	40.19
Stretch vibration H–O–H	–	–	1631.78	99.12	1652.99	94.56	1652.99	94.53
C–OH bending vibration	–	–	1336.67	93.76	1340.52	99.51	1340.52	98.36
C–O–H stretch vibration	–	–	1149.57	82.12	1151.50	94.88	1151.50	90.54
			1076.28	74.96	1078.20	90.18	1078.20	80.41
C–O–C asymmetric stretch	–	–	993.34	50.09	1020.34	84.36	1024.20	74.04
			860.25	86	860.25	99.30	860.25	99.25
			761.88	82.15	763.81	98.07	763.81	97.75
–CH$_2$ bending (shear)	1473.61	76.91	–	–	1462.04	74.82	1462.04	73.72
–CH$_2$-vibration (rocking)	719.44	68.31	–	–	719.44	68.45	719.44	67.13

different compositions are given in Fig. 4a–d with different magnifications (from 257× to 1081×). For the HDPE/starch blends, the surface morphology revealed well-visible dislocated regions similar to spherical particles, representing starch particles and indicating the partial miscibility between the HDPE and starch (Fig. 4a). Increasing starch content to 60% (Fig. 4b) leads to a clearer phase separation on the rupture surfaces (an increase in the degree of phase separation), which can explain the decrease of tensile stress following the increase of starch introduced amount. Figure 4c, d shows the fractured surfaces morphology of the HDPE/starch/linen fiber composites (P60 S30 F10) and (P60 S20 F20), respectively. The micrographs clearly show the fibers dispersion in the atrix composed by HDPE/starch and serving as reinforcement of the composite structure. Furthermore, deformations were also noticed in the matrix surfaces, which is indicative of the low interfacial adhesion. However, no significant pull-out zones, which are common in fibers' composites were observed.

From the previously obtained FTIR spectra and morphological analysis results, it can be inferred that the compatibility between PE and starch is clearly reduced by increasing the starch content in the composite formulation. The introduction of linen fibers into the composite formulation is shown to improve the compatibility by acting as a bridge between starch and PE as can be seen from the P60 S20 F20 micrographs.

Thermogravimetric analysis

Thermogravimetric analysis

Three samples with the best mechanical properties were selected for thermal analysis: pure HDPE (P100), HDPE/starch blend (P60 S40) and HDPE/starch/linen fiber (P60 S20 F20). The TGA curves shown in Fig. 5 represent the variation in the weight loss of the samples with the increasing temperature, which is indicative of their degradation. The thermal decomposition of P100 samples showed only one stage corresponding to the entire weight loss starting at around 416 °C and ending at 500 °C. For the P60 S40 samples, three stages were identified. The first weight loss of the sample (10% at 100 °C) was related to water evaporation, the second (29% at 256 °C) and the third (60% at
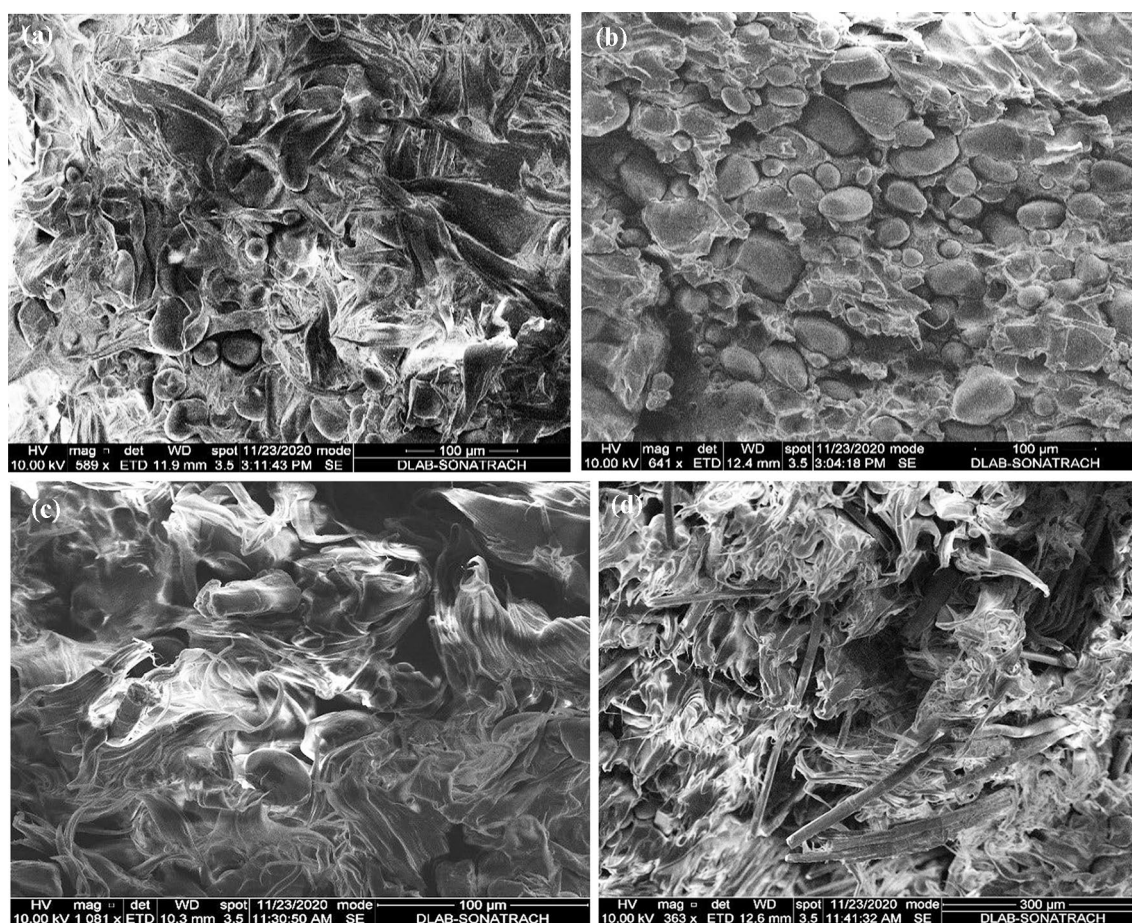

Fig. 4 SEM analysis of fracture surfaces of: **a** P60 S40 F00, **b** P40 S60 F00, **c** P60 S30 F10 and **d** P60 S20 F20
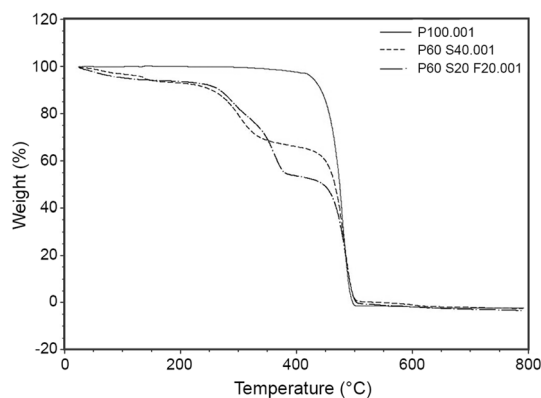
Fig. 5 TGA curves of P100, P60 S40 and P60 S20 F20

446 °C) are due to the thermal decomposition of starch and HDPE, respectively. Similarly, curve for P60 S20 F20 samples exhibited three stages with approximately 10%, 40% and 50% weight loss at about 100 °C, 271 °C and 446 °C and corresponding to water loss, starch and linen degradation, and HDPE decomposition, respectively. Obviously, the thermal decomposition of HDPE is achieved at high temperature, indicating its high stability and, therefore, low degradability. Its thermal stability was superior compared to HDPE/starch and HDPE/starch/linen composites, indicating close agreement with the literature [11, 27]. The thermal stability of HDPE/starch blend and HDPE/starch/linen composite was almost the same up to 350 °C, with only 30% weight loss, but above this value, at 400 °C, it increased from 34% (by wt) for the P60 S40 samples to 46% (by wt) for the P60 S20 F20 samples. These results indicated that the processing and applications of these composites are restricted to a safe temperature of 250 °C not exceeding the degradation temperature of both starch and linen fibers. It has been reported that the thermal stability limit of the composites with lignocellulosic fibers estimated by the temperature associated with the onset of thermal degradation is in the range of 240–355 °C, and are attributed to the decomposition of the lignocellulosic fiber [32]. However, despite this limitation, the decrease of composites thermal degradation, when not leading to inferior mechanical properties, does not necessarily hinder the use of these materials.

Differential scanning calorimetry analysis

The thermal behavior of HDPE, HDPE/starch blend, and HDPE/starch/linen fibers composite was investigated by DSC analysis and their thermograms are shown in Fig. 6. To assess the influence of starch and fiber incorporation into the HDPE matrix on the physical and mechanical properties of the obtained blend and composite, their thermal proprieties (T_c, T_m, dH_m, dH_c, X_c) were determined and are

recapitulated in Table 4. The most important property is crystallinity, which significantly increases intermolecular bonding, enhancing the physical and mechanical properties of these materials, resulting in improved practical performance characteristics. Indeed, compared to the amorphous phase, the crystalline phase of the HDPE remains unaffected during the glass transition, enhances the density, and furthermore tends to increase stiffness and tensile strength, whereas the amorphous phase soften over the glass transition temperature, however, it is more effective in absorbing impact energy [33].

DSC thermograms showed single exothermic and endothermic peaks, which indicated the crystallization and melting processes that occurred during the cooling and heating cycle, respectively. Starch generally has no melting point and its decomposition occurs at high temperature, and therefore, has an impact on the thermal properties of HDPE/starch blend. As it can be seen from Table 4, increasing the starch content from 0% (by wt) to 40% (by wt) resulted in an increase in X_c from 53.87 to 60 and 67%, i.e., a 6.8% increase, and an increase of dH_c and a decrease of dH_m. The higher X_c for PE/starch blend can be explained by the nucleating action of starch for enhancing the crystallization of PE [7, 29]. However, (T_c) and (T_m) of HDPE/starch blends did not change significantly, which is in accordance with the literatures [7, 27]. On the other hand, the introduction of linen fibers from 0% (by wt) to 20% (by wt) into the HDPE/starch blend resulted in a small reduction of X_c from 60.67 to 58.39%, which is a 4.5% increase compared to the HDPE crystallinity. An increase of dH_c and decrease for dH_m were also registered (Table 4). These results revealed that the contribution of starch was more important than that of linen fiber in X_c enhancement. T_m and T_c of PE/starch/fiber composites did not shift regardless to the amount of fiber inserted due to the partial miscibility between components. These findings are consistent with those obtained for LDPE/starch and starch/fiber composites [16, 31].

Mechanical properties

Izod impact test

Impact tests were used in studying the toughness of the prepared composites. Table 5 shows the results of Izod impact strength test. For the samples of HDPE/starch blends with starch content, the impact strength showed a low value (0.170 J) compared to the HDPE value (0.473 J), which is due to the relatively low miscibility of starch with polyethylene [31]. Indeed, imperfections in the sample caused by poor mixing and/or incompatibility between starch and HDPE, acting as a stress riser and reducing the impact energy resulted in the Izod impact test low value. Conversely, the incorporation of linen fibers, however, for
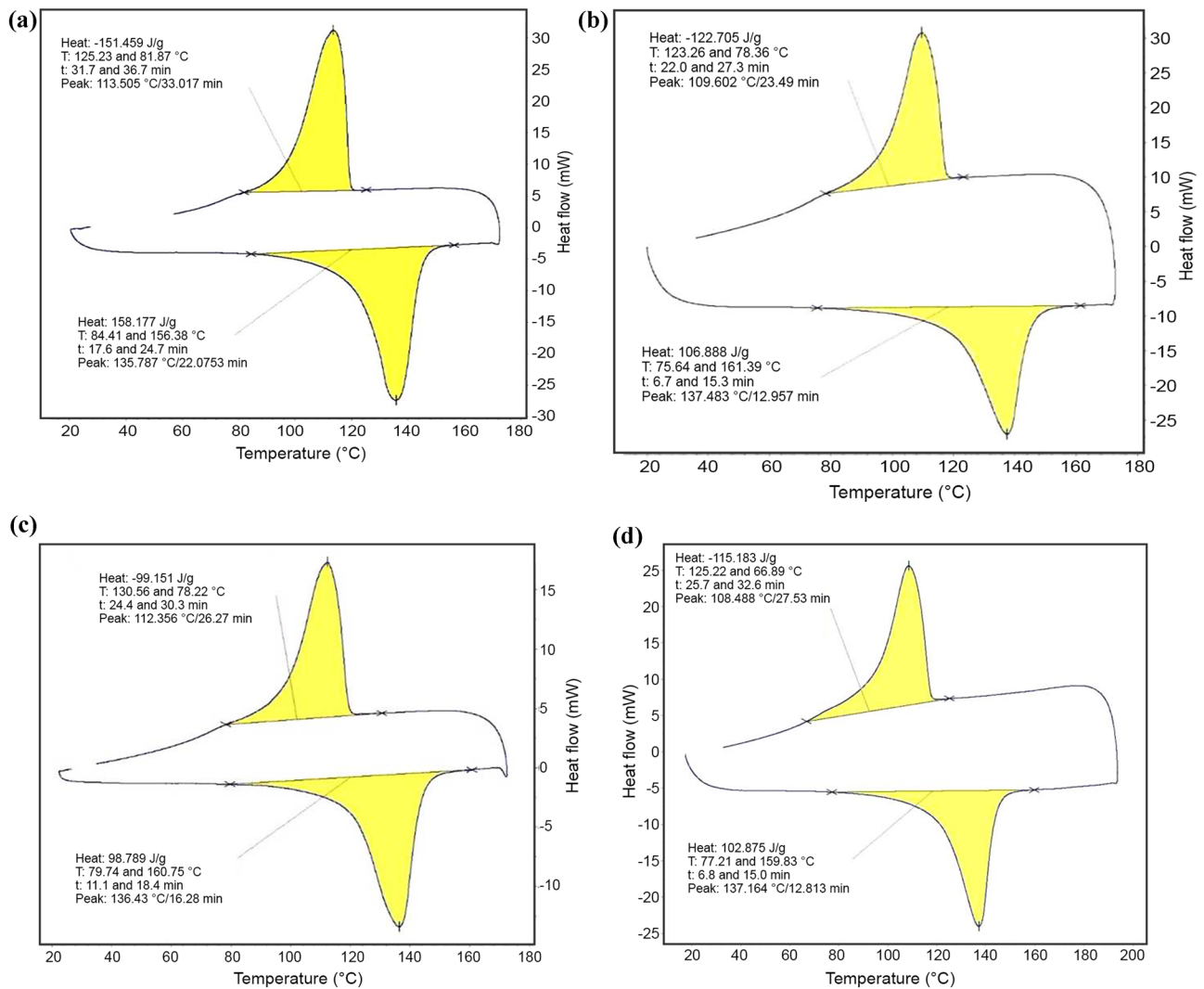
(a)

Heat: -151.459 J/g
T: 125.23 and 81.87 °C
t: 31.7 and 36.7 min
Peak: 113.505 °C/33.017 min

Heat: 158.177 J/g
T: 84.41 and 156.38 °C
t: 17.6 and 24.7 min
Peak: 135.787 °C/22.0753 min

(b)

Heat: -122.705 J/g
T: 123.26 and 78.36 °C
t: 22.0 and 27.3 min
Peak: 109.602 °C/23.49 min

Heat: 106.888 J/g
T: 75.64 and 161.39 °C
t: 6.7 and 15.3 min
Peak: 137.483 °C/12.957 min

(c)

Heat: -99.151 J/g
T: 130.56 and 78.22 °C
t: 24.4 and 30.3 min
Peak: 112.356 °C/26.27 min

Heat: 98.789 J/g
T: 79.74 and 160.75 °C
t: 11.1 and 18.4 min
Peak: 136.43 °C/16.28 min

(d)

Heat: -115.183 J/g
T: 125.22 and 66.89 °C
t: 25.7 and 32.6 min
Peak: 108.488 °C/27.53 min

Heat: 102.875 J/g
T: 77.21 and 159.83 °C
t: 6.8 and 15.0 min
Peak: 137.164 °C/12.813 min

Fig. 6 DSC curves of: **a** P100, **b** P60 S40 F00, **c** P60 S30 F10 and **d** P60 S20 F20

Table 4 Main DSC thermal proprieties for HDPE/starch/linen fiber composites

Sample	T_c (°C)	T_m (°C)	dH_m (j/g)	dH_c (j/g)	X_c(%)
P100 S0 F00	113.505	135.787	158.177	− 151.453	53.87
P60 S40 F00	109.602	137.483	106.88	− 112.705	60.67
P60 S30 F10	112.356	136.43	98.789	− 99.151	56.07
P60 S20 F20	108.488	137.164	102.875	− 115.185	58.39

Table 5 Izod impact of the composites

Sample code	Izod impact (J)
P100 S00 F00	0.473 ± 0.025
P60 S40 F00	0.170 ± 0.014
P60 S30 F10	0.209 ± 0.013
P60 S20 F20	0.302 ± 0.018

HDPE/starch blend increased the impact strength to reach 0.302 J, which is nevertheless slower to HDPE strength value. The linen fibers effect on increased Izod impact can be attributed probably to the fact that Izod hammer, reaching the fibers in the matrix did not break them but made them folded, which increased the energy needed for breakage. It was reported that for the composites with weak interfacial bonding, Izod impact tests commonly result in fiber pull-out and higher energy dissipation [25]. It was also reported that fiber enhanced the impact strength of composites of different compositions [34]. Indeed, the linen fibers acted as a "load transfer medium", which resisted to fracture, enhancing the impact strength of the composite. These findings are consistent with the literature [35].

Table 6 Results of tensile proprieties of composites

Sample code	Tensile stress (MPa)	Young's modulus (MPa)	Elongation-at-break (%)
P100S00F00	26.7 ± 2.26	1031.90 ± 65.78	586.5 ± 50.16
P 60 S40 F00	19.55 ± 1.03	1415.36 ± 46.54	3.47 ± 0.36
P 60 S30 F10	20.1 ± 0.85	1918.34 ± 31.32	2.54 ± 0.15
P 60 S20 F20	21 ± 1.04	2239.69 ± 121.90	2.55 ± 0.21

Tensile properties

Table 6 shows the mechanical properties (tensile strength, modulus, and elongation-at-break) for the different compositions of HDPE/starch/linen fibers. With the increase of starch content from 20 to 40% (by wt), the tensile strength and elongation-at-break decrease considerably, while the Young's modulus increased significantly. This behavior is attributed to the fact that the transition was made from the flexible HDPE with a 586% elongation-at-break and a tensile strength of 26.7 MPa to the stiffened matrix in which the rigid starch was dispersed in HDPE, and whose elongation-at-break and tensile strength at 40% (by wt) starch content, diminished to 3.47% and 19.55 MPa, respectively. In this case, Young's modulus increased from 1032 to 1415 MPa. The effects resulting from the incompatibility between starch hydrophilic molecules and HDPE hydrophobic molecules impacted evidently the mechanical properties of the HDPE/starch blends [31, 36]. Similar results were obtained for polypropylene/starch blends, which exhibited an improvement of Young's modulus with the addition of starch, whereas elongation-at-break as well as maximum strength or hardness decreased [37, 38]. Compared to the values obtained for the blend samples (P60 S40 F00), the composites samples (P60 S30 F10 and P60 S20 F20) exhibited improved tensile strength, elongation-at-break and Young's modulus; the values of 21 MPa, 2.55% and 2240 MPa were, respectively, recorded for the samples P100 S20 F20. The slight increase in the tensile stress of the composites was due the mechanical anchorage provided by the simultaneous blending of the linen fibers and the HDPE/starch matrix. However, the poor interfacial adhesion between the hydrophobic HDPE and the hydrophilic fiber reduced their compatibility and hindered a substantial increase in tensile strengths. Thus, in contrast to the elongation-at-break, the stiffness of the samples was significantly improved by the reinforcement provided by the linen fibers. The Young's modulus increase was more dependent on the linen fibers content than fiber/matrix interface. These findings are in agreement with the literature [10, 25, 39].

According to these results, increasing the starch content in HDPE/starch blend reduced impact strength, tensile stress and elongation-at-break. This impact was presumably due to the low compatibility between the two components with opposite chemical affinities, and counter-balanced by the improved mechanical anchorage provided by the reinforcement of linen fibers in the HDPE/starch/linen fibers composites. The high fracture resistance of the fibers also improved Young's modulus of these composites.

Conclusion

The morphological aspects and the thermal and mechanical properties of the HDPE/starch/linen fiber composite with different starch and fiber contents were investigated. From the FTIR spectra and morphological analysis results, it was found that the compatibility between HDPE and starch was relatively poor, showing some visible dislocated regions, which negatively affected the impact strength, tensile stress and elongation-at-break of the HDPE/starch blend. On the other hand, the stiffness and Young's modulus were improved due to the increase in the degree of crystallinity attributable to the nucleating action of the starch on crystallization. The trend was counter-balanced by the effects of the dispersed fibers in the HDPE/starch matrix, involving a good mechanical anchorage between these compounds and resulting in good mechanical properties despite weak compatibility between the HDPE and the starch. Based on these results, the HDPE/starch/linen fibers with 60:20:20 composition exhibited good thermal and mechanical properties suitable for use in manufacturing and packaging, with the degradation temperature of the starch and linen fibers satisfied.

References

1. John MJ, Thomas S (2008) Biofibres and biocomposites. Carbohydr Polym 71:343–364

2. Ilyas RA, Sapuan SM (2020) Biopolymers and biocomposites: chemistry and technology. Curr Anal Chem 16:500–503

3. Roy SB, Shit SC, Sengupta RA, Shukla PR (2014) A review on bio-composites: fabrication, properties and applications. Int J Innov Res Sci Eng Technol 3:16814–16824

4. Fowler PA, Hughes JM, Elias RM (2006) Biocomposites: technology, environmental credentials and market forces. J Sci Food Agric 86:1781–1789

5. Méité N, Konan LK, Tognonvi TM, Doubi BHG, Gomina M, Oyetola S (2021) Properties of hydric and biodegradability of cassava starch-based bioplastics reinforced with thermally modified kaolin. Carbohydr Polym 254:117322

6. Ramírez-Hernández A, Hernández-Mota CE, Páramo-Calderón DE, Gonzalez-Garcia G, Baez-Garciac E, Rangel-Porrasc G, Vargas-Torresd A, Aparicio-Saguilan A (2020) Thermal, morphological and structural characterization of a copolymer of starch and polyethylene. Carbohydr Res 488:107907

7. Peres AM, Pires RR, Orefice RL (2016) Evaluation of the effect of reprocessing on the structure and properties of low density polyethylene/thermoplastic starch blends. Carbohydr Polym 136:210–215

8. Jakubowicz I (2003) Evaluation of degradability of biodegradable polyethylene (PE). Polym Degrad Stab 80:39–43

9. Angaji MT, Hagheeghatpadjooh HR (2004) Preparation of biodegradable low density polyethylene by starch–urea composition for agricultural applications. Iran J Chem Chem Eng 23:7–11

10. Junior OGS, Melo R, Sales R, Ayres E, Patricio PSO (2017) Processing and characterization of polyethylene/starch/curauá composites: potential for application as thermal insulated coating. J Build Eng 11:178–186

11. Rodriguez-Gonzalez FG, Ramsay BA, Favis BD (2003) High performance LDPE/thermoplastic starch blends: a sustainable alternative to pure polyethylene. Polymer 44:1517–1526

12. Kaboorani A, Gray N, Hamzeh Y, Abdulkhani A, Shirmohammadli Y (2021) Tailoring the low-density polyethylene—thermoplastic starch composites using cellulose nanocrystals and compatibilizer. Polym Test 93:107007

13. Abbott AP, Abolibda TZ, Qu W, Wise WR, Wright LA (2017) Thermoplastic starch–polyethylene blends homogenized using deep eutectic solvents. RSC Adv 7:7268–7273

14. Torres FG, Cubillas ML (2005) Study of the interfacial properties of natural fibre reinforced polyethylene. Polym Test 24:694–698

15. Zhang CW, Li FY, Li JF, Wang LM, Xie Q, Xu J, Chen S (2017) A new biodegradable composite with open cell by combining modified starch and plant fibers. Mater Des 120:222–229

16. Araujo JR, Waldman WR, De Paoli MA (2008) Thermal properties of high density polyethylene composites with natural fibres: coupling agent effect. Polym Degrad Stab 93:1770–1775

17. Rudnik E (2007) Thermal properties of biocomposites. J Therm Anal Calorim 88:495–498

18. Kaewtatip K, Thongmee J (2012) Studies on the structure and properties of thermoplastic starch/luffa fiber composites. Mater Des 40:314–318

19. Ramachandran M, Bansal S, Raichurkar P (2016) Experimental study of bamboo using banana and linen fiber reinforced polymeric composites. Perspect Sci 8:313–316

20. Liang Y, Liu X, Fang K, An F, Li C, Liu H, Qiao X, Zhang S (2021) Construction of new surface on linen fabric by hydroxyethyl cellulose for improving inkjet printing performance of reactive dyes. Prog Org Coat 154:106179

21. Dalbaşi ES, Kayseri GÖ (2021) A research on the comfort properties of linen fabrics subjected to various finishing treatments. J Nat Fiber 18:909–922

22. Bharath B, Kumar GC, Shivanna G, Hussain SS, Chandrashekhar B, Raj BAS, Kumar SA, Girisha C (2018) Fabrication and mechanical characterization of bio-composite helmet. Mater Today Proc Int Conf Adv Mater Appl (ICAMA 2016) 5:2716–2720

23. Taha I, Steuernagel L, Ziegmann G (2007) Optimization of the alkali treatment process of date palm fibres for polymeric composites. Compos Interface 14:669–684

24. Kargarzadeh H, Johar N, Ahmad I (2017) Starch biocomposite film reinforced by multiscale rice husk fiber. Compos Sci Technol 151:147–155

25. Zhao X, Li RKY, Bai SL (2014) Mechanical properties of sisal fiber reinforced high density polyethylene composites: effect of fiber content, interfacial compatibilization, and manufacturing process. Composites 65:169–174

26. Raghavan D (1995) Characterization of biodegradable plastics. Polym Plast Technol Eng 34:41–63

27. Nguyen DM, Do TVV, Grillet AC, Thuc HH, Thuc CNH (2016) Biodegradability of polymer film based on low density polyethylene and cassava starch. Int Biodeterior Biodegrad 115:257–265

28. Amoroso L, Heeley EL, Ramadas SN, McNally T (2020) Crystallisation behaviour of composites of HDPE and MWCNTs: the effect of nanotube dispersion, orientation and polymer deformation. Polymer 20:122587

29. Stark NM, Matuana LM (2004) Surface chemistry changes of weathered HDPE/wood-flour composites studied by XPS and FTIR spectroscopy. Polym Degrad Stab 86:1–9

30. Ma X, Yu J (2004) The plastcizers containing amide groups for thermoplastic starch. Carbohydr Polym 57:197–203

31. Raj B, Sankar KU, Siddaramaiah (2004) Low density polyethylene/starch blend films for food packaging applications. Adv Polym Technol 23:32–45

32. Monteiro SN, Calado V, Rodriguez RJS, Margem FM (2012) Thermogravimetric stability of polymer composites reinforced with less common lignocellulosic fibers—an overview. J Mater Res Technol 1:117–126

33. Vieille B, Albouy W, Chevalier L, Taleb L (2013) About the influence of stamping on thermoplastic-based composites for aeronautical applications. Compos B Eng 45:821–834

34. Yan L, Kasal B, Huang L (2016) A review of recent research on the use of cellulosic fibres, their fibre fabric reinforced cementitious, geo-polymer and polymer composites in civil engineering. Compos B Eng 92:94–132

35. Premnath AA (2019) Impact of surface treatment on the mechanical properties of sisal and jute reinforced with epoxy resin natural fiber hybrid composites. J Nat Fiber 16:718–728

36. Shujun W, Jiugao Y, Jinglin Y (2005) Preparation and characterization of compatible thermoplastic starch/polyethylene blends. Polym Degrad Stab 87:395–401

37. Bagheri R (1999) Effect of processing on the melt degradation of starch-filled polypropylene. Polym Int 48:1257–1263

38. Roy SB, Rmaraj B, Shit SC, Nayak SK (2011) Polypropylene and potato starch biocomposites: physicomechanical and thermal properties. J Appl Polym Sci 120:3078–3086

39. Baghaei B, Skrifvars K, Salehi M, Bashir T, Rissanen M, Nousiainen P (2014) Novel aligned hemp fibre reinforcement for structural biocomposites: porosity, water absorption, mechanical performances and viscoelastic behaviour. Compos Part A Appl Sci Manuf 61:1–12